Generation of multiple Fano resonances in plasmonic panda's eye structures

Yiyuan Guo, **Yiping Huo**, **Xueying Jiang**, **Chen Zhou**, **Yibo Hou**, **Qiqiang Niu**, **Qian He** and **Xiangxiang Hao**

School of Physics and Information Technology, Shaanxi Normal University, Xi'an 710062, People's Republic of China

E-mail: yphuo@snnu.edu.cn

Abstract

A kind of dimer nanostructure similar to panda's eye (P-E), consisting two center biased elliptical rings, is proposed in this paper. The finite element method is used to study the nanostructure with the vertical incident light. The structure exhibits high order magnetic modes and the magnetic modes intensity can be manipulated independently by changing the structure parameters. The intensities of the magnetic dipole and magnetic quadrupole modes can be controlled by changing the angle between two rings and the distance of two cavity centers, respectively. Moreover, when two circular cavities increase simultaneously, the intensity of the magnetic octupole mode increases accordingly. Fano resonance can be induced when the electric mode couples with the magnetic mode. When the radius of the left circular cavity decreases, triple Fano resonance is formed. And when the whole structure is rotated, quintuple Fano resonance can be formed. More interesting, when the radii of the circular cavities of the two elliptical rings increase to 50 and 55 nm, the nanostructure becomes crescent dimer, and the enhancements of magnetic field and electric field reach 38 and 390, respectively. The P-E structure has potential application value in multiwavelength surface enhanced spectroscopy and biochemical sensing.

Keywords: surface plasmon, multiple Fano resonance, intensities of magnetic modes

(Some figures may appear in colour only in the online journal)

1. Introduction

Surface plasmon photonics is a new subject developed by applying surface plasmon technology to the field of photonics. It is the most important part of nano-photonics. Researchers pay much attention to explore the novel effect and mechanism of surface plasmon photonics. Plasmon has a wide application prospect. For example, it can be used to make surface plasmon polaritons components and circuits, nano-waveguides, surface plasmon photon chips, couplers, modulators and switches, subwavelength optical data storage, and super-resolution imaging beyond diffraction limit, etc.

Surface plasmon is essentially an electromagnetic wave [1] generated by collective oscillation of free electrons on metal surface, and it can be divided into two kinds generally. When surface plasmons propagate continuously along the interface between metal and medium, they are called propagating surface plasmons [2]. Another is local surface plasmon [3, 4], which is generated by the interaction of the external field and the free conduction electrons on the plasmonic nanostructure surface. In addition, when the oscillation frequency of the external field and the natural frequency of the surface plasmon satisfy the phase matching condition [5], resonance can be induced and the surface electric and magnetic field intensity are enhanced, which is called surface plasmon resonance [6, 7].

Generally, according to the magnitude of net dipole moment [8], surface plasmon resonance can be divided into bright mode [9–11] and dark mode [12]. Under the excitation of an external field, the mode which can be excited directly and has a larger dipole moment is called the bright mode. The bright mode has larger radiation damping and the charges oscillate in phase [13, 14]. The dark mode cannot be excited directly by the external field, and the dipole moment is approximately zero. Moreover, the radiation damping of the

dark mode is relatively small and the charges oscillate out of phase [15, 16]. The surface plasmon resonance can be also divided into electric mode [17, 18] and magnetic mode [19] according to whether the circulation loop can be formed in the current distribution map. If the current loop can be formed in the current distribution diagram, the plasomon resonance is a magnetic mode, otherwise it is an electric mode.

Fano resonance [20–22] can be interpreted as coherent coupling between electric mode and magnetic mode. The most striking feature of Fano resonance is asymmetry sharp line shape [23, 24]. At the same time, under certain circumstances Fano resonance can contribute to sub-diffraction limit focusing [25], which can enhance the local field, so it has a good application value in the field of meta-lens [26, 27]. In addition, Fano resonance is also highly sensitive to the structure parameters and the refractive index of the external environment, which has a great application prospect in the field of sensors [28]. Based on these advantages of Fano resonance, many groups have carried out extensive research and proposed a variety of nanostructures, such as nanoring dimer nanostructure [29], disk-ring nanostructure [30], crescent-ring nanostructure [31], and dolmen oligomer nanostructure [32, 33], etc. At present, researchers have paid more attention to multiple Fano resonance because it can control light in multi-band. The nano-crescent-elliptical disk structure proposed by Wang *et al* has realized triple local near-field enhanced Fano resonances [34]. The dual-ring/disc cavity structure proposed by Li *et al* can also realize multiple Fano resonance [35].

A silver nanodimer structure similar to panda's eye is proposed in this paper. The nanostructure can generate higher order magnetic modes and realize multiple Fano resonance. The intensities of magnetic modes can be manipulated effectively and independently by changing the nanostructure parameters. When the radius of the circular cavity in the left ring is reduced, a new electric mode can be excited and triple Fano resonance can be induced by the coupling of the electric mode and the magnetic mode. Similarly, when the whole structure is rotated, the quintuple Fano resonance can also be realized. In addition, the intensity of each magnetic mode can be controlled by changing the angle between the axes of two center biased elliptical rings, the center distance of the circular cavities and the radii of the circular cavities, respectively. Finally, when the nanostructure becomes crescent dimer, the electric field and magnetic field can reach 390 and 38 times of the incident field, respectively.

2. Structure and simulation method

The P-E structure is shown in figure 1, which contains two center biased elliptical rings placed symmetrically. The length of the long and short half-axis of the ring are a and b, which are 90 nm and 70 nm, respectively. The center distance of the two cavities is d, and the radii of the inner cavities are defined as r_1 and r_2, respectively. In figure 1(a), p and k points is on the edge of two elliptical rings respectively, so that the straight lines o′p and o″k are parallel to the long axes of the

two elliptical disks respectively. The angle between the straight lines o′p and o″k is defined as θ. The angle between the symmetric axis of the structure and the polarization direction of the incident light is defined as β. Finally, the thickness of the whole nanostructure is expressed by T, and T is 20 nm. The values of a, b and T are fixed throughout the simulation process. In addition, the excitation source is plane electromagnetic wave. Its propagation direction is along the *z*-axis (perpendicular to the nanostructure), and the polarization direction of the electric field is along the *x*-axis. The whole simulation process is carried out by using COMSOL multi-physics software. Moreover, the sweep frequency range of the whole calculation process is 400–1800 nm. The whole nanostructure has a perfect matching layer design outside, and the structure is surrounded by air. In noble metal materials, silver has the excellent properties of minimum loss and absorption coefficient [36], so silver is used as the material of the P-E. The sum of absorption cross section and scattering cross section is extinction cross section [37].

3. Results and discussion

3.1. The spectral properties of the P-E nanostructure

Figure 2 shows the extinction cross section when $d = 120$ nm, $\theta = 120°$ and $r_1 = r_2 = 40$ nm. Four distinct plasmon resonance peaks can be seen, namely, electric dipole mode E_1, magnetic dipole mode M_1, magnetic quadrupole mode M_2 and magnetic octupole mode M_3. Because of the interference coupling between E_1 and M_1, a Fano resonance is formed at D_1.

In order to further verify the results, the charge and current distributions of E_1, M_1, M_2 and M_3 are shown in figure 3. It can be seen that the E_1 mode has a larger electric dipole moment and no current loop, so it is an electric mode. For M_1, M_2, M_3, it can be seen that they all have obvious circulation loop from the current density and magnetic field distribution, so they are called magnetic modes. In addition, from the charge distribution diagram, M_1 is a magnetic dipole mode, M_2 is a magnetic quadrupole mode and M_3 is a magnetic octupole mode. Finally, due to the coupling of electric dipole E_1 and magnetic dipole M_1, a Fano dip D_1 is formed.

3.2. Generation of multiple Fano resonance by changing the radius of the circular cavity in the left elliptical ring

We also study the optical properties of the structure when r_1 is reduced. And the corresponding extinction spectra are shown in figure 4(a). When r_1 is decreased to 30 nm, mode E_2 is stimulated for the broken symmetry of the nanostructure. As r_1 decreases, the asymmetry of the nanostructure increases and the intensity of mode E_2 increases gradually. The charge and current distributions of mode E_2 with $r_1 = 0$ nm are shown in figures 4(b) and (c). It can be found that there is no obvious current loop in mode E_2, so it is an electric mode. Because of the coherent coupling between the electric mode
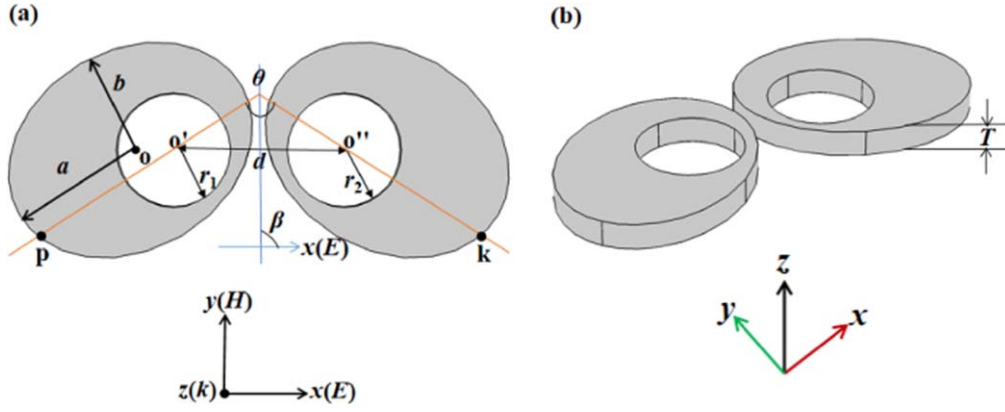
Figure 1. (a) 2D graph of the P-E nanostructure and the geometrical parameters. (b) 3D graph of the P-E.
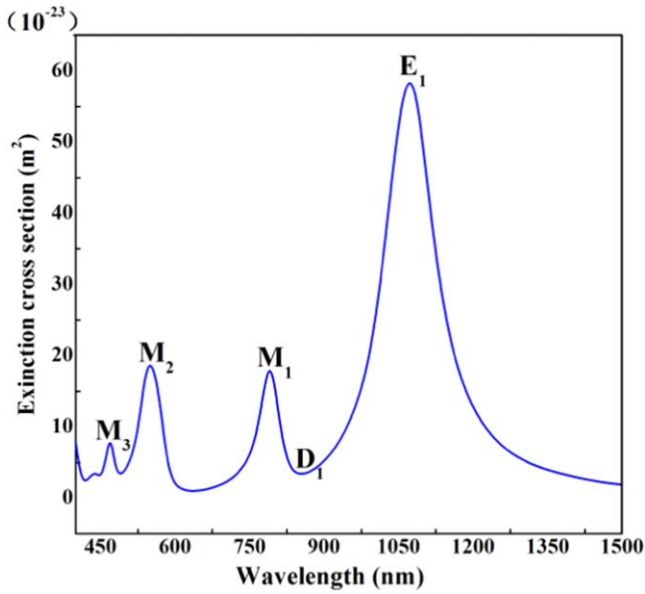
Figure 2. The extinction cross section of the P-E, where $d = 120$ nm, $\theta = 120°$ and $r_1 = r_2 = 40$ nm.

and the magnetic mode, triple Fano resonance is formed in the extinction spectrum.

3.3. Generation of multiple Fano resonance by rotating the whole nanostructure

In addition, we also study and discuss the extinction spectra of the whole nanostructure when it is rotated at different angles. It is found that multiple Fano resonance can also be induced when the whole nanostructure is rotated and the extinction spectra are shown in figure 5(a). The angle between the nanostructure symmetry axis and the polarization direction of the incident light is defined as β. When β is 10°, electric mode E_3 appears. When β is 30°, magnetic mode M_2 splits into electric mode E_4 and magnetic mode M_2. That is to say, the electric mode E_3 and electric E_4 are caused by the increase of the angle β.
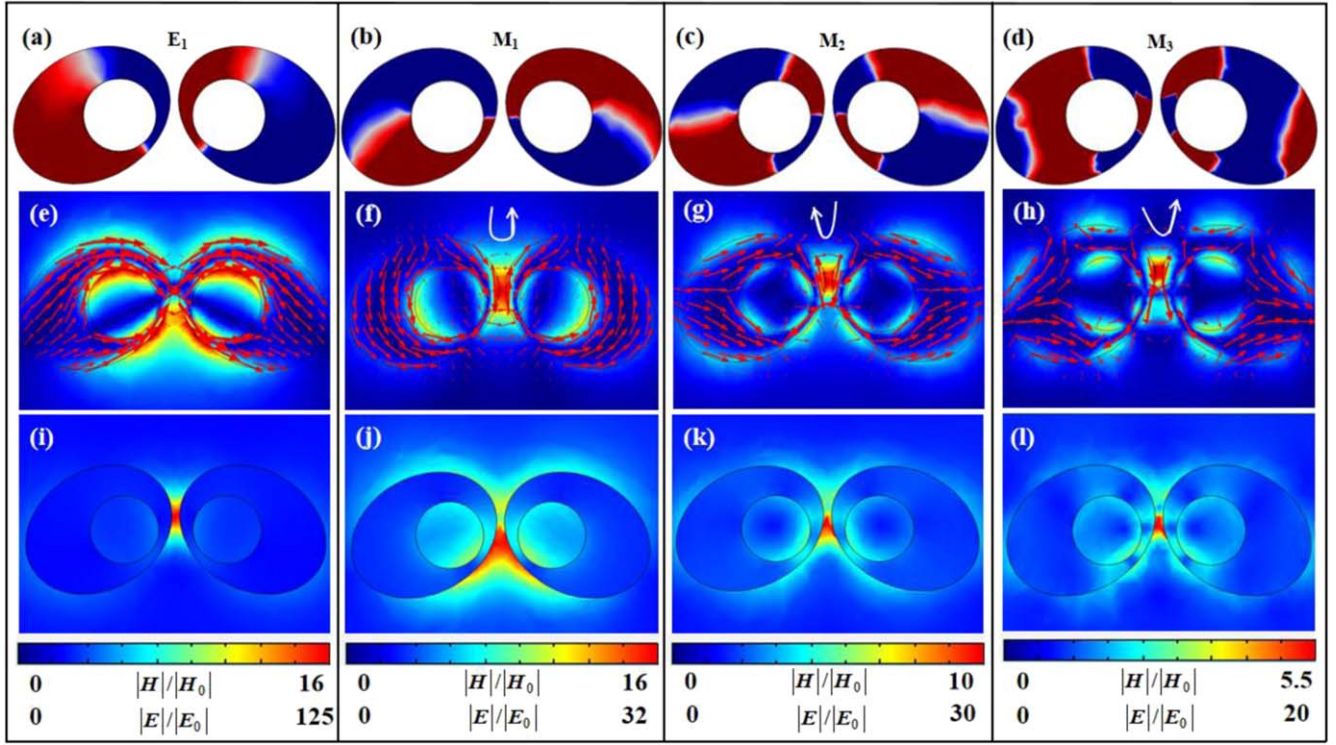
Figures 5(b) and (c) show the charge distributions of electric mode E_3 and E_4 when the nanostructure is rotated

40°, respectively. Figures 5(d) and (e) show the current distribution and magnetic field enhancement of electric mode E_3 and E_4, respectively. We can see from the current distribution that neither E_3 nor E_4 modes have current loops, so they are all electric modes. In this way, when the structure is rotated 40°, five Fano dips are generated in the extinction spectrum, which makes the structure realize quintuple Fano resonance. Multiple Fano resonance is conducive to controlling and tuning light in multi-band. And the P-E can be used to nonlinear optical resonance [38], surface Raman spectroscopy [39] and advanced biosensor technology [28].

3.4. Intensity manipulation of plasmon resonance mode independently

The intensities of magnetic dipole mode M_1, magnetic quadrupole mode M_2 and magnetic octupole mode M_3 can be controlled by changing the nanostructure parameters independently. Firstly, as the two elliptical disks rotate around o′ and o″, respectively, the angle θ increases ($d = 120$ nm and $r_1 = r_2 = 40$ nm). Figure 6(a) shows the extinction spectra of the P-E with different θ. We can find that when θ decreases from 140° to 60°, the coupling between the two rings increases, which account for the intensity enhancement of magnetic dipole mode M_1. From figure 6(d), it can be found that in the range of 140°–60°, the intensity of magnetic dipole mode M_1 increases fast and is almost linearly with the decrease of angle θ. Secondly, as shown in figure 6(b), magnetic quadrupole mode M_2 is excited, when the distance d decreases and θ, r_1, r_2 remain unchanged. The intensity of M_2 increases with the decrease of distance d, which are due to the increase of coupling intensity between the two circular cavities. As can be seen from figure 6(e), the intensity of magnetic quadrupole mode M_2 increases linearly with the decrease of distance d. Thirdly, figure 6(c) shows the extinction spectra of magnetic octupole mode M_3 with different r, here $r_1 = r_2 = r$. When r increases, and θ, d remain unchanged, the coupling between the circular cavities and the outer edge of the elliptical rings increases, so the intensity of magnetic octupole mode M_3 also increases. From figure 6(f), it is can be seen that the intensity of magnetic octupole mode M_3 decreases first and then increases as r increases. Here, the

Figure 3. (a)–(d) The charge distributions of mode E_1, M_1, M_2 and M_3. (e)–(h) The current density and magnetic field enhancement distributions of mode E_1, M_1, M_2 and M_3. (i)–(l) The electric field enhancement distributions of mode E_1, M_1, M_2 and M_3.
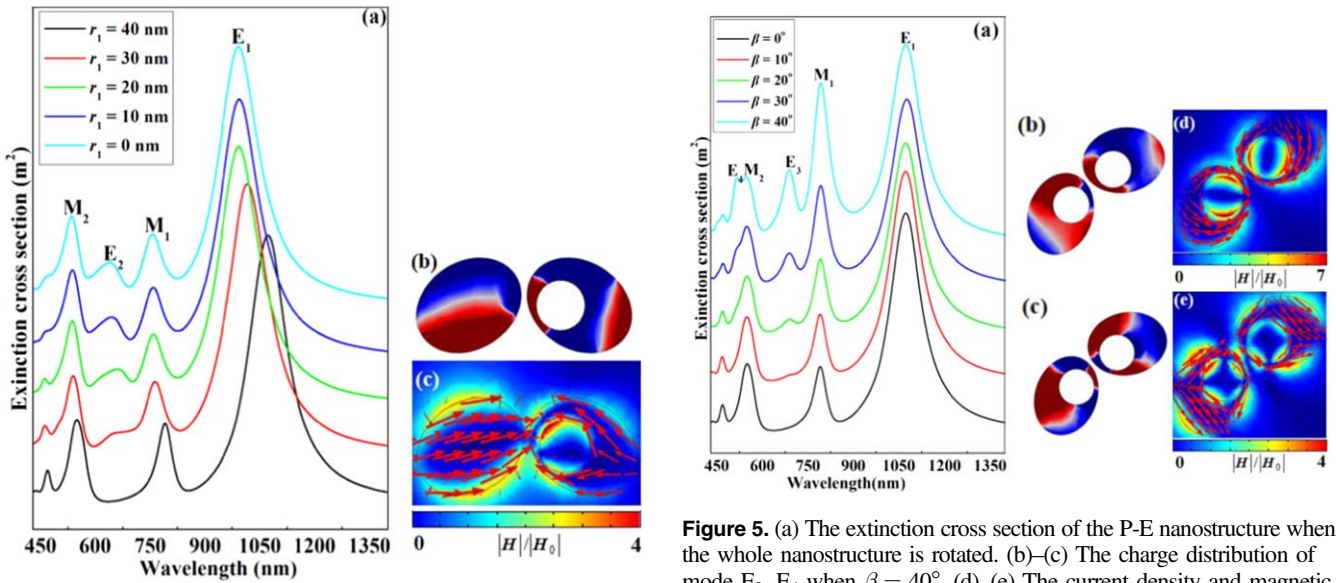
Figure 4. (a) The extinction cross section of the P-E nanostructure when the radius of the left circular cavity decreases. (b) The charge distribution of mode E_2 when $r_1 = 0$ nm. (c) The current density and magnetic field enhancement distribution of mode E_2 when $r_1 = 0$ nm.
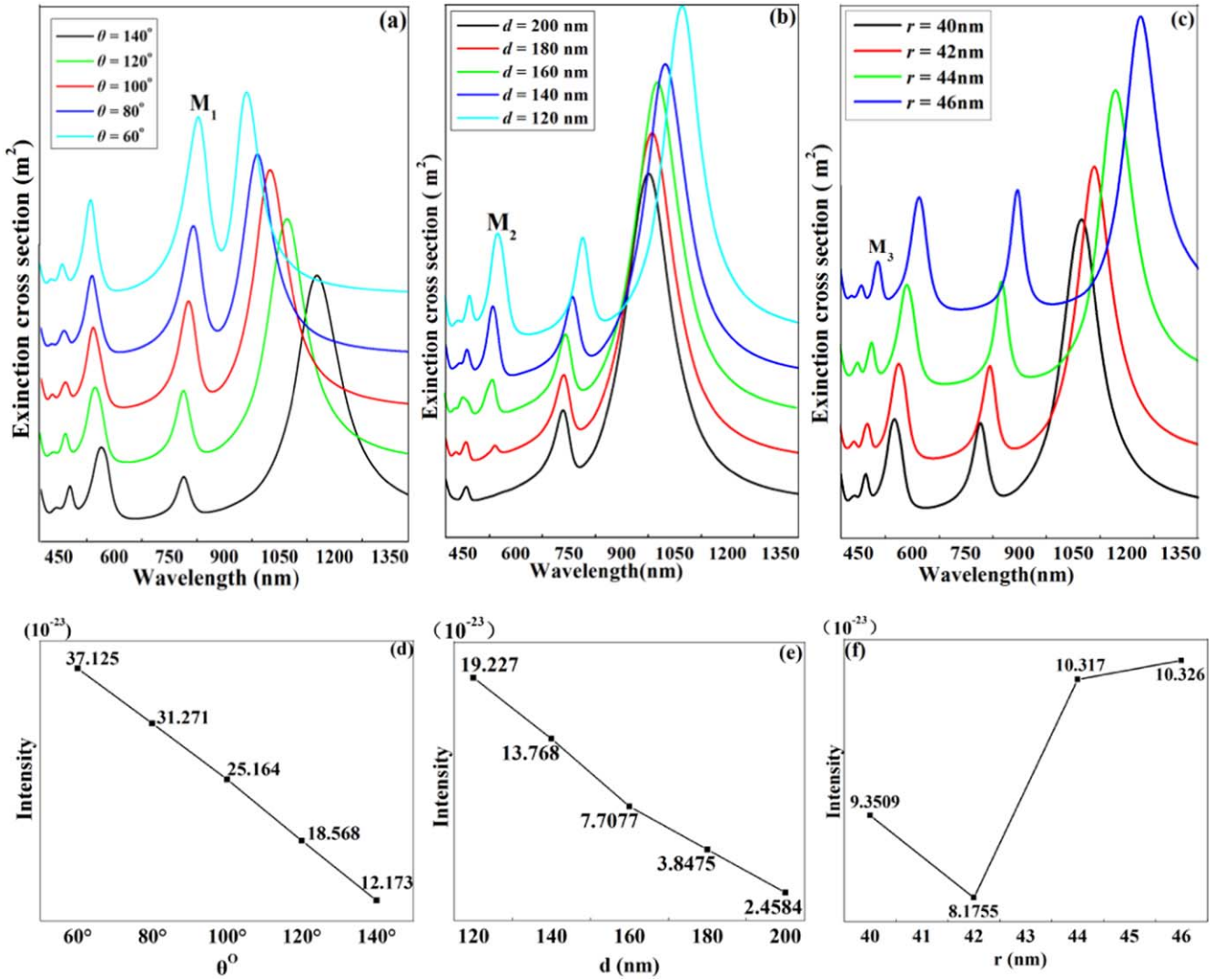

Figure 5. (a) The extinction cross section of the P-E nanostructure when the whole nanostructure is rotated. (b)–(c) The charge distribution of mode E_3, E_4 when $\beta = 40°$. (d)–(e) The current density and magnetic field enhancement distribution of mode E_3, E_4 when $\beta = 40°$.

intensity decrease of magnetic octupole mode M_3 may be due to the destructive interference. In addition, we can also find that modes M_1, M_2 and M_3 have only a slight red shift with the decrease of θ, d and the increase of r, respectively. In conclusion, the intensity of mode M_1, M_2 and M_3 can be enhanced by decreasing θ, decreasing d and increasing r_1 and r_2, respectively.

3.5. Enhancement of the electric field and magnetic field by increasing the radii of the two circular cavities

Here, the radii r_1 and r_2 further increased and the extinction spectra of the P-E are studied. When r_1 and r_2 are increased to 50 nm, the nanostructure becomes crescent dimer. For the
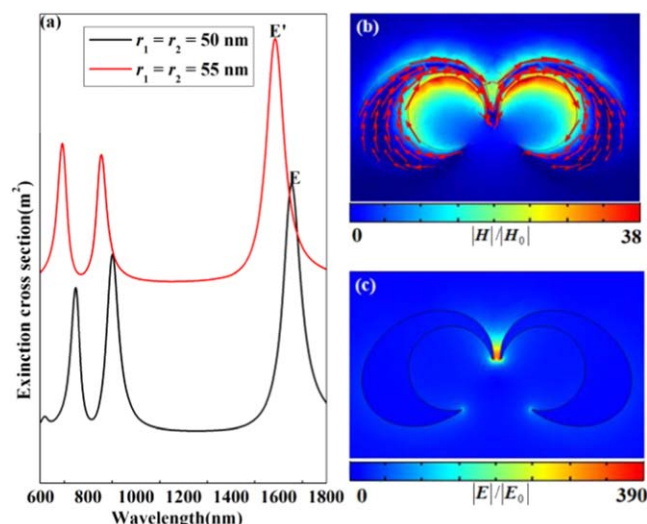
Figure 6. (a) The extinction cross section of the P-E nanostructure when θ is changed. (b) The extinction cross section of the P-E nanostructure when d is changed. (c) The extinction cross section of the P-E nanostructure when r_1 and r_2 are changed synchronously. (d)–(f) The diagrams of extinction intensity changes of mode M_1, M_2 and M_3, respectively.

crescent dimer nanostructure, relevant researchers have done in-depth research [40, 41], the crescent dimer nanostructure proposed in this paper is expected to be very good application in near-field enhancement. Figure 7(a) shows the extinction spectra when the radii of the two circular cavities increases to 50 and 55 nm. Figures 7(b) and (c) denote magnetic field and electric field enhancement distributions when $r_1 = r_2 = 50$ nm and $r_1 = r_2 = 55$ nm, respectively. It is found that when r_1 and r_2 are 50 nm, the magnetic field intensity of resonance E increases 38 times as much as the incident field. When r_1 and r_2 are 55 nm, the electric field enhancement of resonance E' is 390 times that of the incident field. The magnetic field enhancement is caused by the breaking of the circular cavity, and the electric field enhancement is the result of the tip coupling of two crescents. It can be seen from figure 3 that the maximum electric field enhancement of P-E structure is 125 times of the incident light, and the maximum magnetic field enhancement is 16 times of the incident light. It is obvious that the field enhancement value of crescent dimer structure is large.

4. Conclusion

In this paper, the nanostructure of Panda's Eyes is proposed and studied. Electric mode E_2 can be generated by reducing r_1, while electric mode E_3 and E_4 can be excited by rotating the whole structure. Because of the coupling of electric mode and magnetic mode, the triple Fano resonance and the quintuple Fano resonance can be obtained. In addition, by changing the size of nanostructure's parameters, such as θ, d, and r, the magnetic resonance modes M_1, M_2 and M_3 can be enhanced respectively, which makes the nanostructure hopeful for practical application. Finally, by further increasing the radii of the circular cavities, the nanostructure becomes a crescent dimer. And when the radii of the circular cavities in the two rings are increased to 50 nm, the magnetic field can be enhanced 38 times as much as the incident field. When the radii of the circular cavities are increased to 55 nm, the electric field can be enhanced 390 times as much as the incident field. Compared with the field enhancement diagrams

Figure 7. (a) The extinction cross section of the P-E nanostructure when $r_1 = r_2 = 50$ nm and $r_1 = r_2 = 55$ nm. (b) The magnetic field enhancement distribution of mode E when $r_1 = r_2 = 50$ nm. (c) The electric enhancement distribution of mode E′ when $r_1 = r_2 = 55$ nm.

of the P-E nanostructure (figure 3), the electric field of the crescent dimer is more than 3 times that of the P-E nanostructure, and the magnetic field is more than 2 times that of the P-E nanostructure. In a word, the P-E nanostructure proposed in this paper has great potential application in multiwavelength surface enhanced spectroscopy and biochemical sensing.

Acknowledgments

ORCID iDs

Yiyuan Guo ⬤ https://orcid.org/0000-0002-7317-7267
Yiping Huo ⬤ https://orcid.org/0000-0002-0013-9593
Xueying Jiang ⬤ https://orcid.org/0000-0002-6749-4178
Chen Zhou ⬤ https://orcid.org/0000-0001-8146-4082
Yibo Hou ⬤ https://orcid.org/0000-0002-5061-7207
Qiqiang Niu ⬤ https://orcid.org/0000-0003-2024-2982
Qian He ⬤ https://orcid.org/0000-0002-8983-1710
Xiangxiang Hao ⬤ https://orcid.org/0000-0003-1873-0055

References

[1] Jamid H A and Albader S J 1995 Diffraction of surface plasmon-polaritons in an abruptly terminated dielectric-metal interface *IEEE Photonics Technol. Lett.* **7** 321–3

[2] Shen X, Cui T J, Martincano D and Garciavidal F J 2013 Conformal surface plasmons propagating on ultrathin and flexible films *Proc. Natl Acad. Sci. USA* **110** 40–5

[3] Boltasseva A 2008 Efficiency of local surface plasmon polariton excitation on ridges *Phys. Rev.* B **78** 115115

[4] Murray W, Auguié B and Barnes W L 2009 Sensitivity of localized surface plasmon resonances to bulk and local changes in the optical environment *J. Phys. Chem.* C **494** 5120–5

[5] Zhang X and Forrest S R 2010 Generalized phase matching condition for lossy periodic photonic structures *Opt. Express* **18** 1151

[6] Homola J, Yee S S and Gauglitz G 1999 Surface plasmon resonance sensors: review *ABC* **377** 528–39

[7] Hutter E and Fendler J 2010 Exploitation of localized surface plasmon resonance *Adv. Mater.* **16** 1685–706

[8] Jiang X *et al* 2019 Double Fano resonances and electromagnetically induced transparency-like optical response achieved by breaking the symmetry of two double-split rings *Phys. Scr.* **94** 8

[9] Sun G *et al* 2017 *Q*-factor enhancement of Fano resonance in all-dielectric metasurfaces by modulating meta-atom interactions *Sci. Rep.* **7** 8128

[10] Liu T T *et al* 2017 Fano resonances of a ring-shaped 'hexamer' cluster at near-infrared wavelength *Physica* B **533** 63–8

[11] Qiu R *et al* 2018 Tunable multipolar fano resonances and electric field enhancements in Au ring-disk plasmonic nanostructures *Materials* **11** 1576

[12] Cao W, Singh R, Zhang C and Han J 2013 Plasmon-induced transparency in metamaterials: active near field coupling between bright superconducting and dark metallic mode resonators *Appl. Phys. Lett.* **103** 917

[13] HongJin H *et al* 2018 Fano resonances with a high figure of merit in silver oligomer systems *Photonics Res.* **6** 204

[14] Liu J T, Liu Z and Hu H F 2019 Tunable multiple Fano resonance employing polarization-selective excitation of coupled surface-mode and nanoslit antenna resonance in plasmonic nanostructures *Sci. Rep.* **9** 2414

[15] Tanatar B and Vignale G 2005 Out-of-phase plasmons in double-layer electron systems (presented to the MAR05 Meeting of the American Physical Society.)

[16] Nguyen T T and Shklovskii B I 2001 Adsorption of charged particles on an oppositely charged surface: oscillating inversion of charge *Phys. Rev.* E **64** 041407

[17] Bakhti S *et al* 2016 Fano-like resonance emerging from magnetic and electric plasmon mode coupling in small arrays of gold particles *Sci. Rep.* **6** 32061

[18] Wang J *et al* 2013 Double Fano resonances due to interplay of electric and magnetic plasmon modes in planar plasmonic structure with high sensing sensitivity *Opt. Express* **21** 2236–44

[19] Sheikholeslami S N, Garci A-Etxarri A and Dionne J A 2011 Controlling the interplay of electric and magnetic modes via fano-like plasmon resonances *Nano Lett.* **11** 3927–34

[20] Luk'Yanchuk B *et al* 2010 The fano resonance in plasmonic nanostructures and metamaterials *Nat. Mater.* **9** 707

[21] Miroshnichenko A E, Flach S and Kivshar Y S 2009 Fano resonance in nanoscale structures *Rev. Mod. Phys.* **82** 2257–98

[22] Rahmani M, Luk'Yanchuk B and Hong M 2013 Fano resonance in novel plasmonic nanostructures *Laser Photonics Rev.* **7** 329–49

[23] Kumar 2013 Asymmetry to symmetry transition of fano line-shape: analytical; description *Indian J. Phys.* **87** 49–52

[24] Wang F *et al* 2009 Fano-resonance-based mach-zehnder optical switch employing dual-bus coupled ring resonator as two-beam interferometer *Opt. Express* **17** 7708–16

[25] Chen S, Jin S and Gordon R 2014 Subdiffraction focusing enabled by a fano resonance *Phys. Rev.* X **4** 1767–70

[26] Yiting Y *et al* 2018 An investigation of influencing factors on practical sub-diffraction-limit focusing of planar super-oscillation lenses *Nanomaterials* **8** 185

[27] Roy T, Rogers E T and Zheludev N I 2013 Sub-wavelength focusing meta-lens *Opt. Express* **21** 7577–82

[28] Rich R L and Myszka D G 2000 Advances in surface plasmon resonance biosensor analysis *Curr. Opin. Biotechnol.* **11** 54–61

[29] Nana Koya A, Ji B, Hao Z and Lin J 2016 Controlling optical field enhancement of a nanoring dimer for plasmon-based applications *J. Opt.* **18** 055007

[30] Xiao J J, Qiang Z and Xiao M Z 2014 Interaction between single nano-emitter and plasmonic disk-ring nanostructure with multiple Fano resonances *J. Opt. Soc. Am.* B **31** 2193–220

[31] Xiao F, Zhu W, Premaratne M and Zhao J 2014 Controlling fano resonance of ring/crescent-ring plasmonic nanostructure with bessel beam *Opt. Express* **22** 2132

[32] Zhang S, Genov D A, Wang Y, Liu M and Zhang X 2008 Plasmon-induced transparency in metamaterials *Phys. Rev. Lett.* **101** 047401

[33] Verellen N *et al* 2009 Fano resonances in individual coherent plasmonic nanocavities *Nano Lett.* **9** 1663–7

[34] Wang Q, Yu L, Liu C and Xu X 2017 Enhancement of multipolar fano resonances by nanocrescent elliptical disk structures *EPL* **118** 64002

[35] Jing L, Yi Z, Jia T and Sun Z 2014 High tunability multipolar fano resonances in dual-ring/disk cavities *Plasmonics* **9** 1251–6

[36] Rycenga M *et al* 2011 Controlling the synthesis and assembly of silver nanostructures for plasmonic applications *Chem. Rev.* **111** 3669–712

[37] Hlaing M, Gebear-Eigzabher B, Roa A, Marcano A, Radu D and Lai C Y 2016 Absorption and scattering cross-section extinction values of silver nanoparticles *Opt. Mater.* **58** 439–44

[38] Jia Y, Shan Y, Leiming W U, Dai X, Fan D and Xiang Y 2018 Broadband nonlinear optical resonance and all-optical switching of liquid phase exfoliated tungsten diselenide *Photonics Res.* **6** 58–65

[39] Ru E C L and Etchegoin P G 2009 *Principles of Surface-enhanced Raman Spectroscopy* (Elsevier) pp 655–663

[40] Fischer *et al* 2011 Plasmon hybridization and strong near-field enhancements in opposing nanocrescent dimers with tunable resonances *Nanoscale* **3** 4788–97

[41] Zhang X M *et al* 2014 Plasmonic supermodes in nanocrescent dimer with tunable resonances at the near-infrared *Opt. Commun.* **325** 9–14